RSC Advances

ROYAL SOCIETY OF CHEMISTRY

www.rsc.org/advances

RSC Advances

Recent advances in biological applications of cage metal complexes

Yan Z. Voloshin*, Valentin V. Novikov, Yulia V. Nelyubina

Nesmeyanov Institute of the Organoelement Compounds, Russian Academy of Sciences, Moscow, Russia. E-mail: voloshin@ineos.ac.ru

1. Introduction

Modern technologies heavily rely on the knowledge from different fields of science. Today, novel pharmaceuticals, diagnostic methods and materials, such as biological/non-biological constructs [1], are being constantly produced at the crossroads of biology, materials engineering, biochemistry and synthetic chemistry. Until recently, the main efforts of medicinal chemists have been focused on creating new potent drugs within the realm of organic chemistry; however, over the last decade, the need for pharmaceuticals with improved potency and selectivity has shifted the attention of some researchers towards metal complexes [2]. Advantages they provide over purely organic compounds are structural diversity [3], simple synthesis and specific characteristics, such as redox [4], optical [5], catalytic [6], radioactive [7] and magnetic [8], induced by a metal ion.

Whereas some medicinal applications of metal complexes, e.g. catalytic transformations in living organisms [9], require the metal ion to be easily accessible by biological environment, other approaches may benefit from its total isolation, which may help to ensure stability of a biologically-active complex by avoiding its decomposition, transmetallation or unwanted coordination. An intuitive strategy in this case is to bury the metal ion inside a three-dimensional ligand, as in cage complexes (clathrochelates [10]). Encapsulation of a transition metal ion leads to complexes with high chemical stability and unusual properties that can be used as molecular scaffolds for new (photo)electronic devices (molecular switches [11], magnetic [12] and electrochromic [13] materials), molecular machines [14], electrocatalysts for hydrogen production [15], metallomacrocycles [16], metalorganic frameworks [16b] and coordination capsules [17].

Biological applications of clathrochelates have been covered previously in 1995 [18] and 2007 [19]. This short review summarizes the progress that has been made in this area since then. First, biological aspects of clathrochelates will be addressed for which the role of the metal ion is purely structural, so all their activity owes to the caging ligand. Then applications will be

highlighted that take advantage of the encapsulated metal ion itself: those include the use of clathrochelates as radioactive and magnetic probes for diagnostics and therapy.

2. Topological drugs: cage metal complexes as rigid scaffolds for macromolecular binding

The most biologically active agents bind to biological targets by either covalent bonds or supramolecular interactions; their selectivity and specificity determine the performance of these agents in drug therapy. Modern trends in drug development lead to the discovery of new biological targets, hidden allosteric sites (that is, compounds residing in special allosteric centres far from the active site of an enzyme cause a change in its properties) and interfaces of macromolecular interactions.

A recent concept of "allosteric drugs" [20] implies the presence of hidden allosteric sites in nearly all the existing proteins, thus offering opportunities for developing agents that inhibit them as shown in Scheme 1**a**. These sites are usually not known, and their choice depends heavily on the ability to create artificial molecules that are topologically complementary to them. Another modern approach in drug therapy is targeting protein–protein interactions; given a rather extensive surface of macromolecular interfaces, the modulation of these interactions requires relatively small but bulky inhibitor molecules of suitable size (Scheme 1**b**).

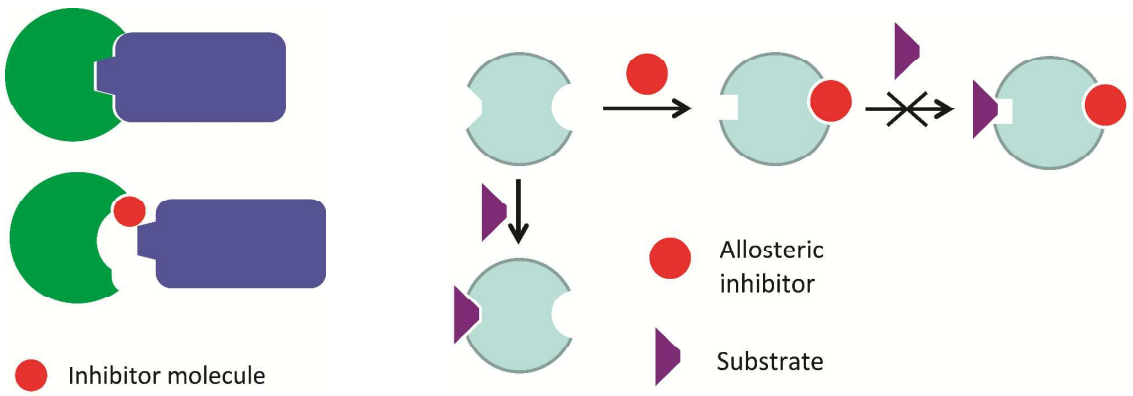

Scheme 1. Inhibition of macromolecular protein – protein interactions by interface (**a**) and allosteric (**b**) inhibitors.

These new biological targets demand for new guest molecules with tunable geometry and extensive surface [21]. A concept [22], for which the term "topological drugs" has been coined [21], suggests the use of rigid three-dimensional species that form multicentered supramolecular interactions in vacant cavities of protein macromolecules and of their complexes. Among polyhedral and cage compounds (Figure 1), transition metal clathrochelates [10], fullerenes [23],

carboranes and metallacarboranes [24] are large and bulky enough to ensure strong multicentered supramolecular binding by van der Waals interactions with large protein molecules. Design of the topological drugs paves the way towards new antitumor and antiviral drug candidates; it is also possible that drug resistance is less likely to develop in this case, if it is caused by enzymatic deactivation of the active compound.

Clathrochelate-based xenobiotics, which have neither natural analogs nor structural similarity to biological molecules, are of particular interest. An example of xenobiotics among polyhedral compounds is derivatives of adamantane carbocycle (Figure 1) widely used in drug therapy of Parkinson's and other human viral, dermatological and psychical diseases. The activity of these compounds is usually attributed to the bulky carbocyclic polyhedron that allows them to be included into lipid bilayers of biological membranes and to interact with biological targets such as hydrophobic parts of proteins. Therefore, the therapeutic effects of these diamonoids are governed by their geometric complementarity to the corresponding receptors [25].

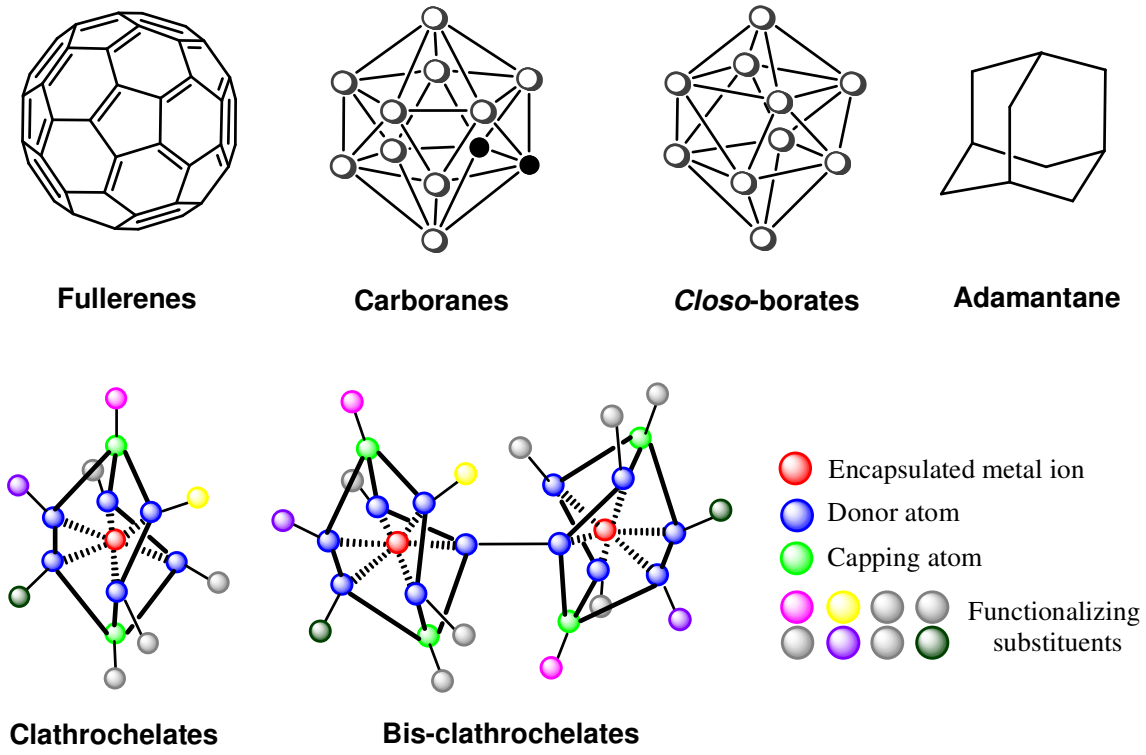

Figure 1. Polyhedral and cage metal compounds.

Clathrochelates [10] are topological analogs of the above polyhedral compounds. The applicability of these chemically robust cage complexes, in particular, polyazomethine macrobicyclic tris-dioximates, as possible drug candidates also owes to their synthetic availability and structural diversity; apical (at the green balls on Figure 1) and ribbed (at the blue balls on Figure 1) functionalization of clathrochelates can be easily performed by well-known

organic reactions from commercially available chemical reagents. A typical synthetic pathway to metal clathrochelates (Scheme 2) is by template condensation of α-dioxime with a Lewis-acidic trigonal boron compound and a metal salt [10].

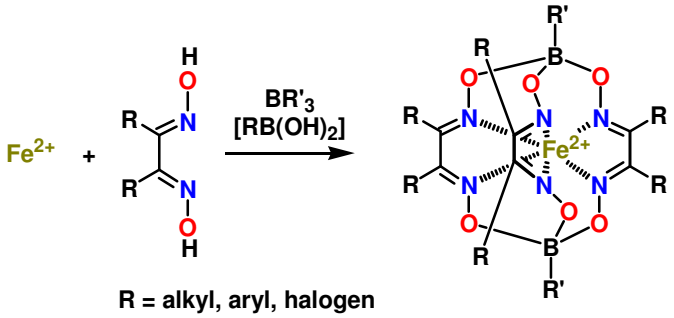

Scheme 2. An exemplary synthetic pathway to transition metal clathrochelates.

Various functionalizing substituents may be introduced into ribbed fragments of a clathrochelate by *N,O,S,P,C*–nucleophilic substitution of halogen atoms in halogenoclathrochelates (Scheme 3); this can produce mono- and triribbed-functionalized cage complexes from mono- [26], di- [27] and hexa- [28] substituted halogenoclathrochelates.

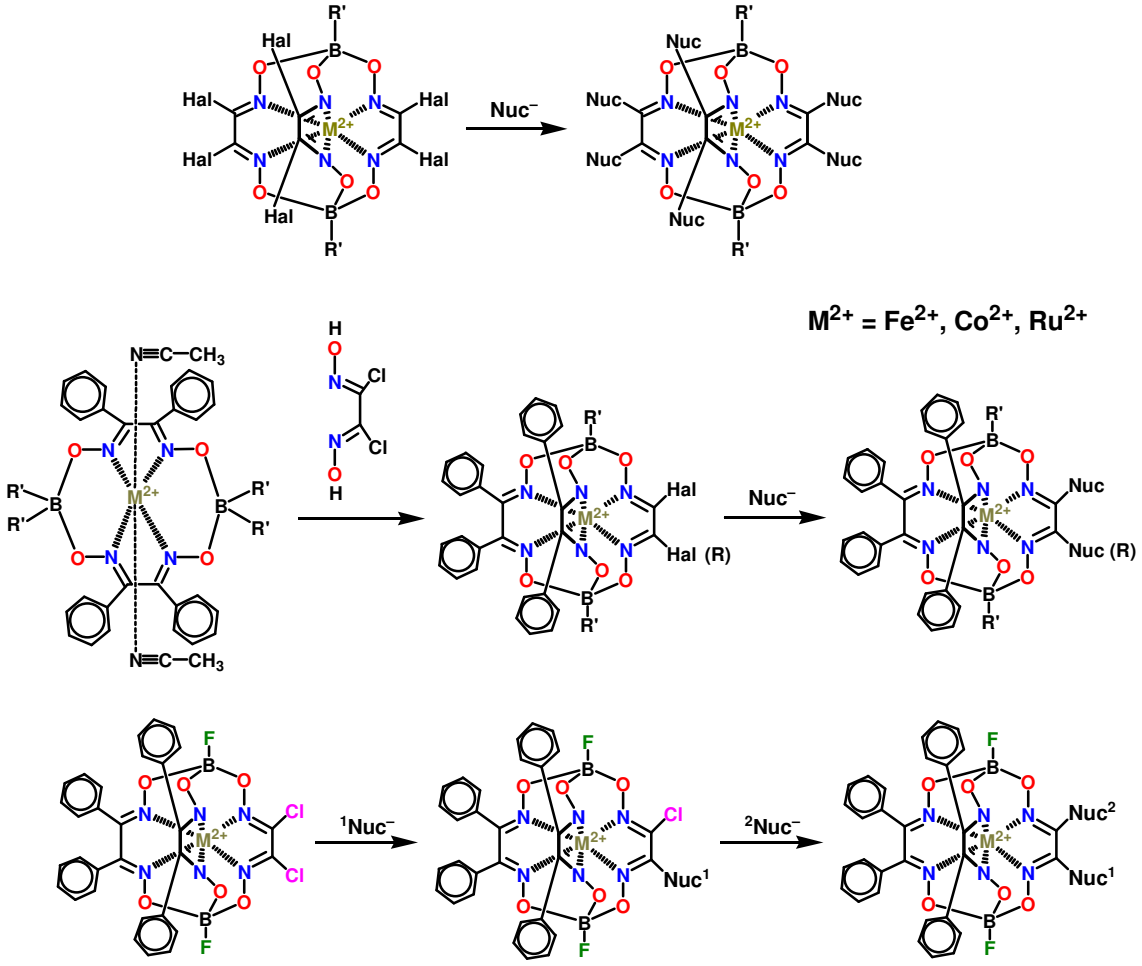

Scheme 3. Functionalization of transition metal clathrochelates.

The possibility to "build" a cage complex from a single center in all directions simultaneously (Figure 1), combined with a wide range of available functionalizing groups (including pharmacophore fragments), allows designing active compounds with shapes closely matching macromolecular surfaces of a very complex topology (such as protein – protein and protein – DNA interaction interfaces) to ensure effective binding of biological macromolecules that affect structure and functions thereof [21].

Binding proteins

Among a series of iron(II) mono- and bis-clathrochelates (Scheme 4), the compounds **7**, **8** and **18** have been tested for binding to bovine serum albumin (BSA), β-lactoglobulin, lysozyme and insulin [29] by steady-state and time-resolved fluorescent spectroscopies. Quenching of the protein's fluorescence and decrease in its excited state lifetime has been observed only in case of BSA, which was an evidence for strong assemblies being formed by the clathrochelates with serum albumins and not with other globular proteins [29].

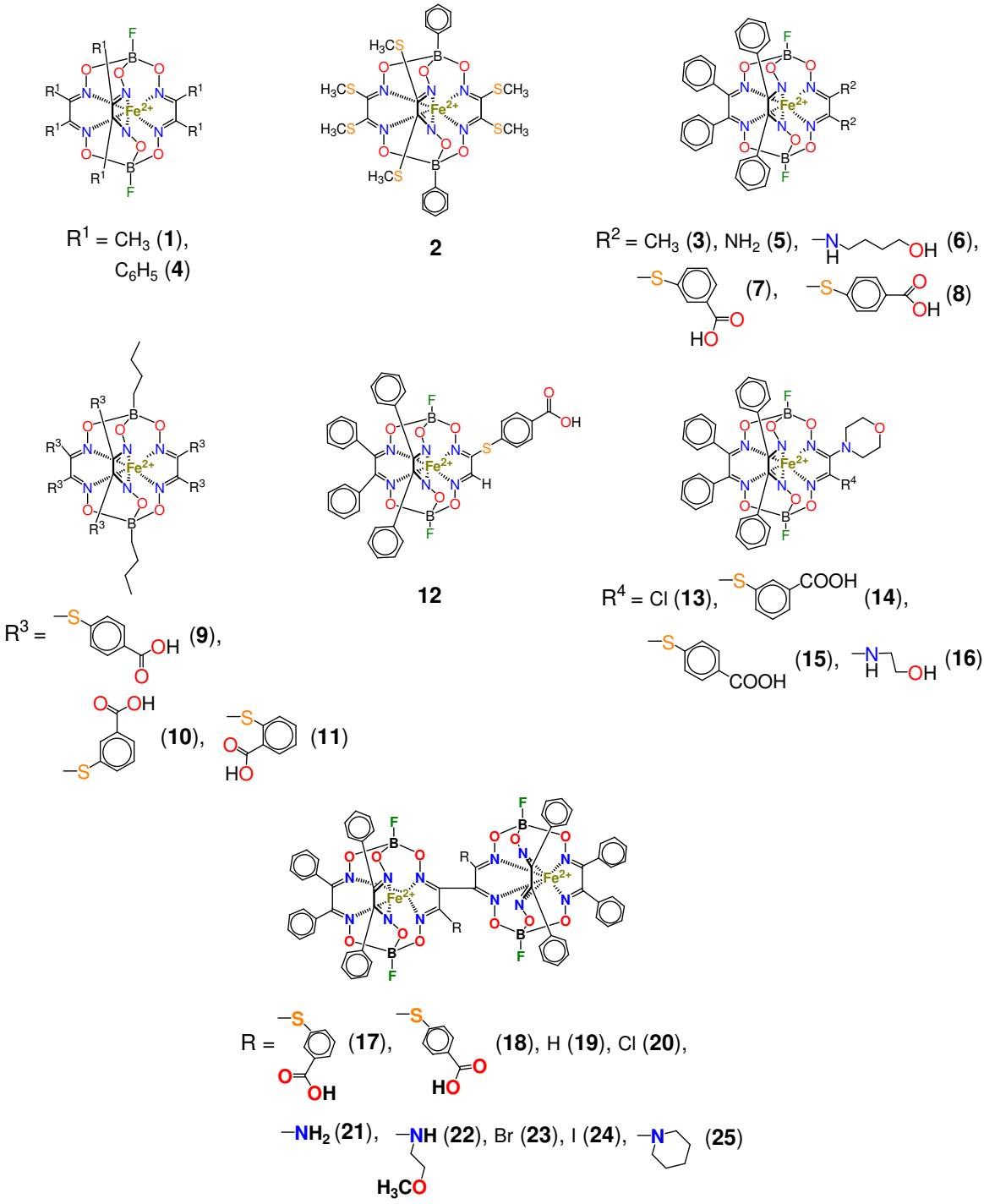

Scheme 4. Iron(II) mono- and bis-clathrochelates with reported biological activity.

Binding of a metal clathrochelate, zinc(II) diaminosarcophaginate **26** (Scheme 5), to bovine and human serum albumins (BSA and HSA) has been explored [30] under simulated physiological conditions. The observations from fluorescent spectroscopy have shown this cage complex to effectively quench intrinsic fluorescence of BSA and HSA *via* static quenching process. Binding sites and binding constants, thus identified and supported by molecular

docking, have suggested that the binding process occurred *via* hydrogen bonding and van der Waals interactions between the clathrochelate and the BSA or HAS species.

The same experimental and theoretical approaches have been used [31] for studying the binding of manganese(II) sarcophaginate **27** (Scheme 5) to these proteins *in vitro*. FT-IR data obtained have shown the conformations of the proteins and their microenvironments to change in the presence of **27**; the latter strongly quenched their intrinsic fluorescence by static quenching. Hydrogen bonding and weak van der Waals interactions have been found to play a key role in stabilizing the resulting clathrochelate–protein supramolecular assemblies. Note that the initial diaminosarcophagine (a caging ligand with no metal ion trapped inside) have also exhibited good binding properties towards HSA and BSA with relatively high binding constants; according to FT-IR data, the secondary protein structures [32] have slightly changed upon that.

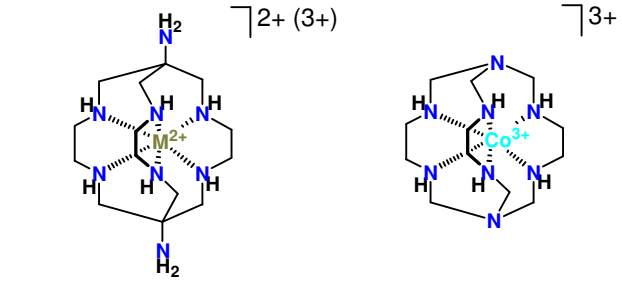

M^{2+} = Zn^{2+} (**26**), Mn^{2+} (**27**), Cu^{2+} (**75**), Cr^{3+} (**76**)

28

Scheme 5. Transition metal sarcophaginates with reported biological activity.

A library of iron(II) tris-dioximate clathrochelates has been screened for inhibitory activity against HIV protease *in silico* [33]. The binding of the leader compound has been observed to occur in an unusual mode, with the cage complex located at the periphery of the protein's cavity rather than at the catalytic aspartate diad, as was expected.

Targeting protein–DNA interactions

The first example of efficient transcription inhibition by a transition metal clathrochelate has been reported for a model *in vitro* system based on a T7 RNA polymerase (T7 RNAP), a small single-subunit polymerase that was often used as a convenient and reliable model in search for transcription inhibitors [34]. The *in vitro* testing of iron(II) clathrochelates **1**–**8** (Scheme 5) in the transcription assay has demonstrated structure- and concentration-dependent inhibition by most of them. Among these complexes, two monoribbed-functionalized iron(II) clathrochelates **7** and **8,** the derivatives of *meta*- and *para*-mercaptobenzoic acids, have been found to suppress the transcription of T7 RNA in a submicromolar range. Heterofunctionalized iron(II) clathrochelates

14 – **16** with good ADMET properties [26c], e.g. sufficient water solubility, membrane permeability and low toxicity, have also demonstrated good inhibitory activity in their low- and submicromolar concentration range.

A series of cobalt(II) bis(1,2-dicarbollides) have been recognized as effective HIV protease inhibitors [35]. To increase their activity even further, it was proposed to join two identical polyhedral fragments by a flexible linker [36]; the resulting construct displayed the activity that was twice as high. A similar approach employing close and relatively rigid joining of two identical clathrochelate frameworks (Scheme 6) has been used to obtain a clathrochelate-based inhibitor having a vastly expanded binding surface with a relatively low increase in conformational flexibility [37]. The C–C conjugated bis-clathrochelates thus obtained have inhibited the transcription in the T7 RNAP system extremely efficiently, with values of IC_{50} below the submicromolar range; this places them among the most potent metal-based transcription inhibitors to date [37a]. Although having limited torsion mobility around the C–C bond that links the two cage frameworks, these bis-clathrochelates were able to accommodate their geometry to match the shape of the binding site, while keeping the number of conformational states low to ensure higher selectivity [37a].

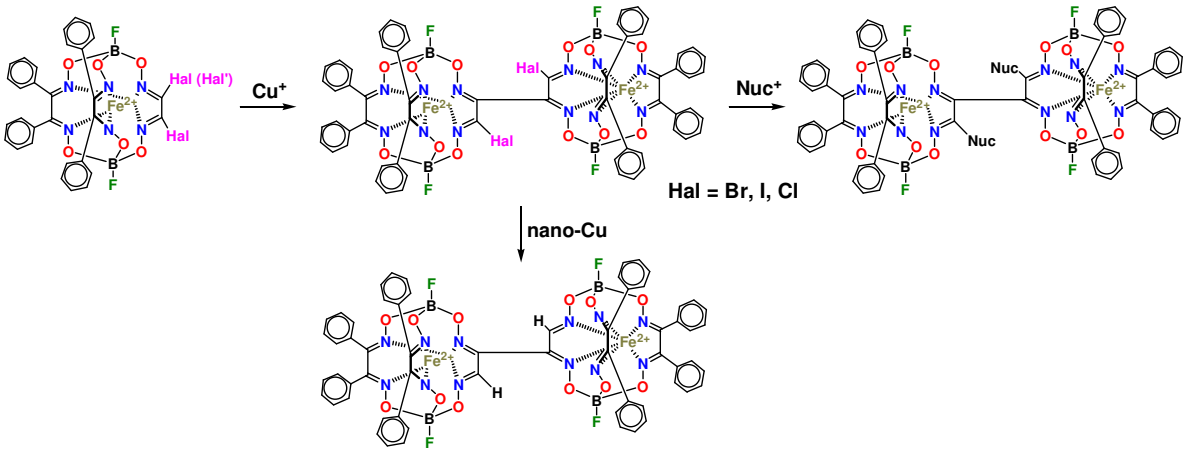

Scheme 6. Synthesis of C – C conjugated iron(II) bis-clathrochelates.

Binding of the above iron(II) mono- and bis-clathrochelates (Scheme 4) to T7 RNAP has been found *in silico* [26c, 34a, 37a] to occur *via* occupying the same region of a macromolecular complex – in the transcriptional bubble – and involving intermolecular contacts with protein residues as well as with DNA and RNA. The clathrochelate molecule resided in the pocket formed by the surfaces of DNA and RNA and completed by the two structural elements of T7 RNAP that interacted with its phenyl substituents, thus trapping the clathrochelate molecule inside. The inhibition of the transcription in this system was ensured by blocking further strand separation *via* binding of the clathrochelate in the transcription bubble to give a quaternary

complex that was able interfere with the translocation step of this reaction. This has been confirmed by preincubation of the leader compound with DNA, with T7 RNAP and with their mixture [34a]; the experimental data have been in a good agreement with the theoretical results from molecular docking, all suggesting the DNA–RNAP complex (or yet a DNA–RNA–RNAP ternary complex) as a target for these clathrochelate-based inhibitors. The observed mode of inhibition by the mono- and bis-clathrochelates that involved a binding pocket formed by three interconnected macromolecules of the transcription complex has been attributed [34a, 37a] to their rather unique structural features: these complexes are large enough to ensure efficient binding mostly by van der Waals interactions; this binding mode seems to be less probable for small and planar molecules.

Targeting protein–protein interactions

Transition metal clathrochelates have only recently emerged as anti-fibrillogenic agents [38] to fight neurodegenerative disorders (such as Alzheimer's, Parkinson's and Creutzfeldt–Jakob's), type II diabetes and amyloidosis, all caused by the deposition of insoluble protein β-pleated formations (aggregates or amyloid fibrils) in cells and extracellular space of various organs or tissues. Addition of the iron(II) mono- and bis-clathrochelates **7**, **8** and **17** (Scheme 4) to an *in vitro* system with insulin has significantly changed the kinetics of insulin fibrillization, reduced the amount of fibrils formed (up to 70%) and caused a decrease in their diameter to 3–8 nm from 5–12 nm typical for free insulin fibrils. These complexes also prevented lateral aggregation of mature fibrils and formation of superfibrillar clusters. The highest inhibitory activity has been observed for the monoclathrochelate derivative of the *meta*-mercaptobenzoic acid **7**: its efficient inhibitory concentration IC_{50} was as low as 16±2 μM [38].

Targeting DNA–DNA interactions

A transition metal clathrochelate, cobalt(III) sepulchrate **28** (Scheme 5), has been reported to promote DNA condensation [39] by forming macromolecular complexes with several molecules of DNA. This clathrochelate effectively precipitated DNA at high concentrations, thus emerging as a much more efficient condensation agent than its non-macrocyclic analogues. Although electrostatic interactions are the main driving force for binding of multivalent complex cations (as a sepulchrate cation) to DNA in a solution, the process of DNA condensation also depends on their structure; supramolecular recognition and consequent DNA condensation by such cations are affected by changes in their size, chemical composition and surface [39].

3. Cage complexes for radiation therapy and diagnostics

Nuclear medicine uses radiation to provide diagnostic information on how specific organs function or to treat them**.** A recent development of nuclear medicine, Positron Emission Tomography (PET) [40], is a more precise functional imaging technique used mostly for identifying medical conditions (including cancers, heart disease and brain disorders) or following the progress of their treatment.

Among transition metals that can be buried in a boron-based macrobicyclic ligand to produce a clathrochelate, those that provide radioisotopes useful for this purpose include copper and cobalt. Isotopes of copper ^{60}Cu, ^{61}Cu, ^{62}Cu and ^{64}Cu are positron emitters with half-life ranging from relatively short (9.74 minutes for ^{62}Cu) to relatively long (12.7 hours for ^{64}Cu) [40b, 41]. The long half-life of ^{64}Cu allows using this isotope for PET imaging as well as for radiotherapy; selectivity and target delivery of the ^{64}Cu isotope to a biological organ are very important for its radiopharmaceutical applications.

Biodistribution of $^{64}Cu^{2+}$ complexes is governed by their stability, size, shape, charge, lipophilicity and redox properties, and further selectivity can be achieved using vector substituents that bind to specific molecular targets *in vivo* [40b]. Among copper(II) clathrochelates, sarcophaginates functionalized by biologically relevant groups have been recognized as promising candidates for future PET imaging agents [42]. Scheme 7 shows a synthetic pathway to a copper(II) sarcophaginate **29** to be turned into a sarcophagine **30** specifically designed [43] for binding to peptides. Functionalization of polyamine macrobicyclic ligands (such as sarcophagines) is a real challenge, as they have eight reactive centers (two apical primary and six ribbed secondary amino groups) resulting in a poorly separable mixture of clathrochelate products.

In the copper(II) sarcophaginate **29**, the donor secondary amino groups are deactivated by their coordination to the encapsulated metal ion. The demetallation of this intermediate complex gave a monofunctionalized aminosarcophagine **30**, which then underwent condensation with a cyclic peptide. The resulting sarcophagine **31** allowed a target delivery of its $^{64}Cu^{2+}$ complex [43]. The latter may also be synthesized with no need for the isolation of an intermediate copper(II) sarcophaginate **29** [44]. In this case, the intermediate sarcophagine to be further functionalized has been obtained from a corresponding cobalt(III) cage complex by either its demetallation followed by base hydrolysis of the free ligand or by its base hydrolysis followed by demetallation (Scheme 8).

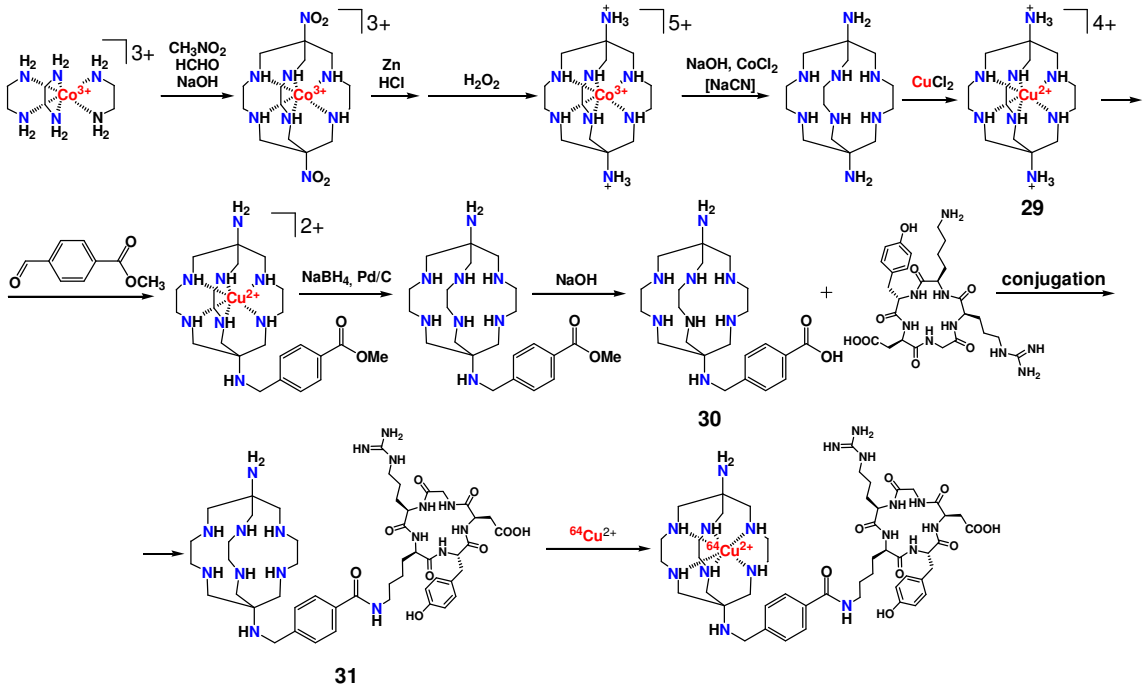

Scheme 7. Synthesis of a copper(II) complex with sarcophagine **31**.

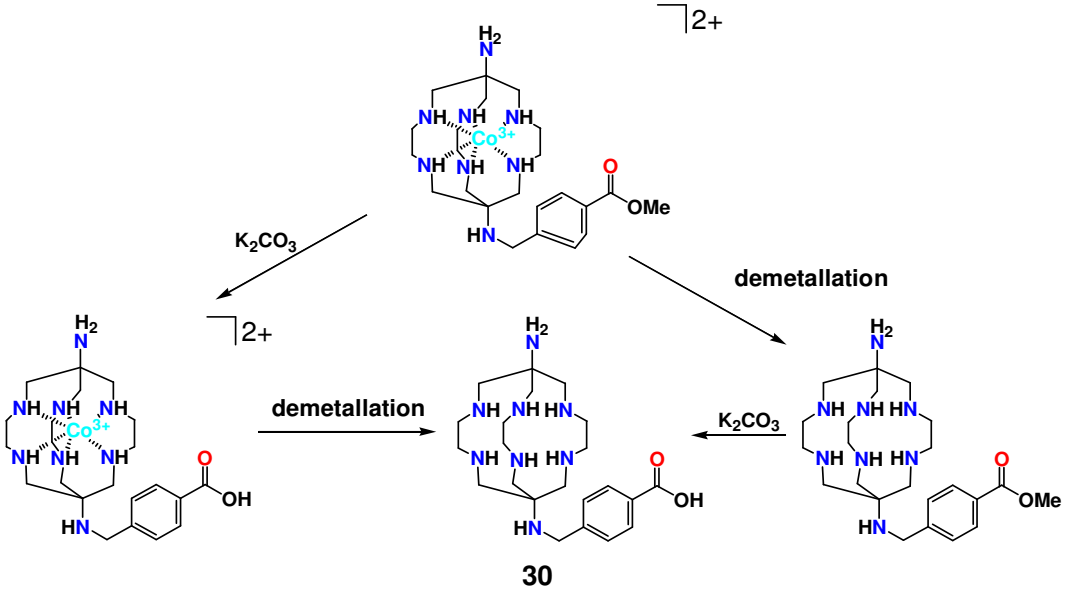

Scheme 8. Synthesis of a carboxyl-terminated sarcophagine **30**.

An analogous bifunctionalized sarcophagine **32** (Scheme 9) has been synthesized [45] by direct alkylation of its diaminosarcophagine precursor with 4-bromobenzoic acid. Its condensation with the corresponding peptide gave a sarcophagine **33**, the copper $^{64}Cu^{2+}$ complex of which showed an uptake by tumor cells exceeding that for the sarcophaginate of **30**. Note that a $^{68}Ga^{3+}$-encapsulating analogue [46] turned out to be a promising non-invasive PET imaging agent.

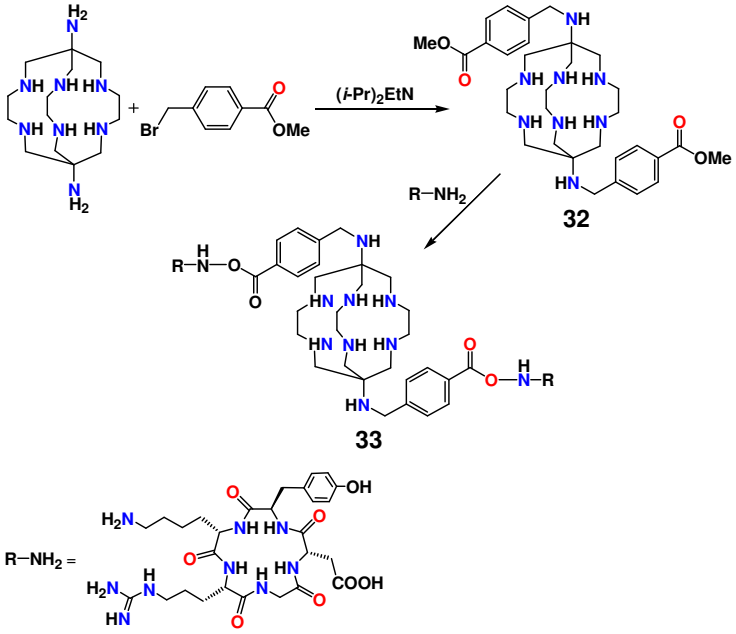

Scheme 9. Synthesis of a sarcophagine **32** and its peptide conjugate **33**.

Mono- and bifunctionalized copper(II) sarcophaginates **34** – **36** (Scheme 10) with di- or trimethylene linkers and with terminal reactive carboxylic groups [47] have been obtained from octaamine precursors; their further functionalization with various peptides has allowed obtaining $^{64}Cu^{2+}$ sarcophaginates that were stable for a long time under the conditions of *in vivo* experiments [48]. Another sarcophaginate-based bioconjugate **38** (Scheme 11) with the encapsulated $^{64}Cu^{2+}$ ion, which performed well in both *in vitro* and *in vivo* experiments [49], has been synthesized *via* 1,3-dipolar cycloaddition of a dibenzocyclooctyne-functionalized $^{64}Cu^{2+}$ sarcophaginate **37** with an azide-containing cyclic peptide.

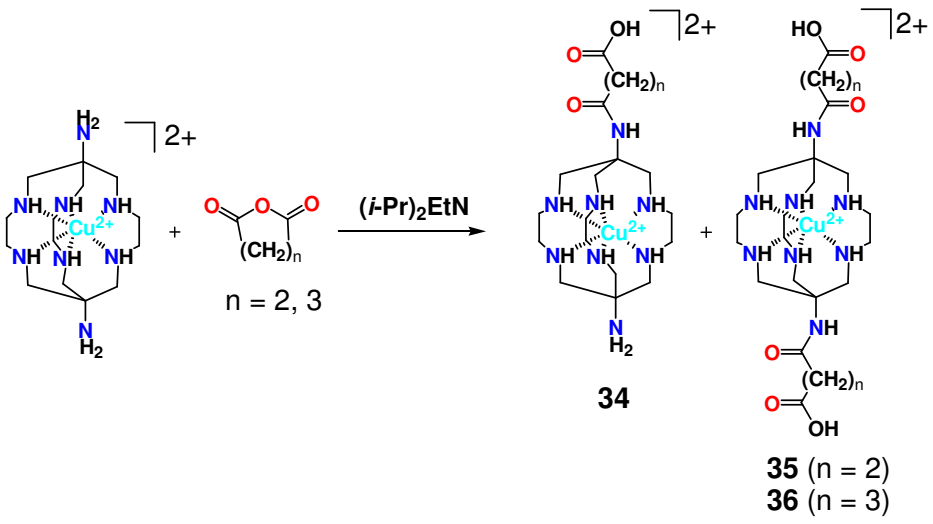

Scheme 10. Synthesis of mono- and bifunctionalized copper(II) sarcophaginates **34** – **36**.

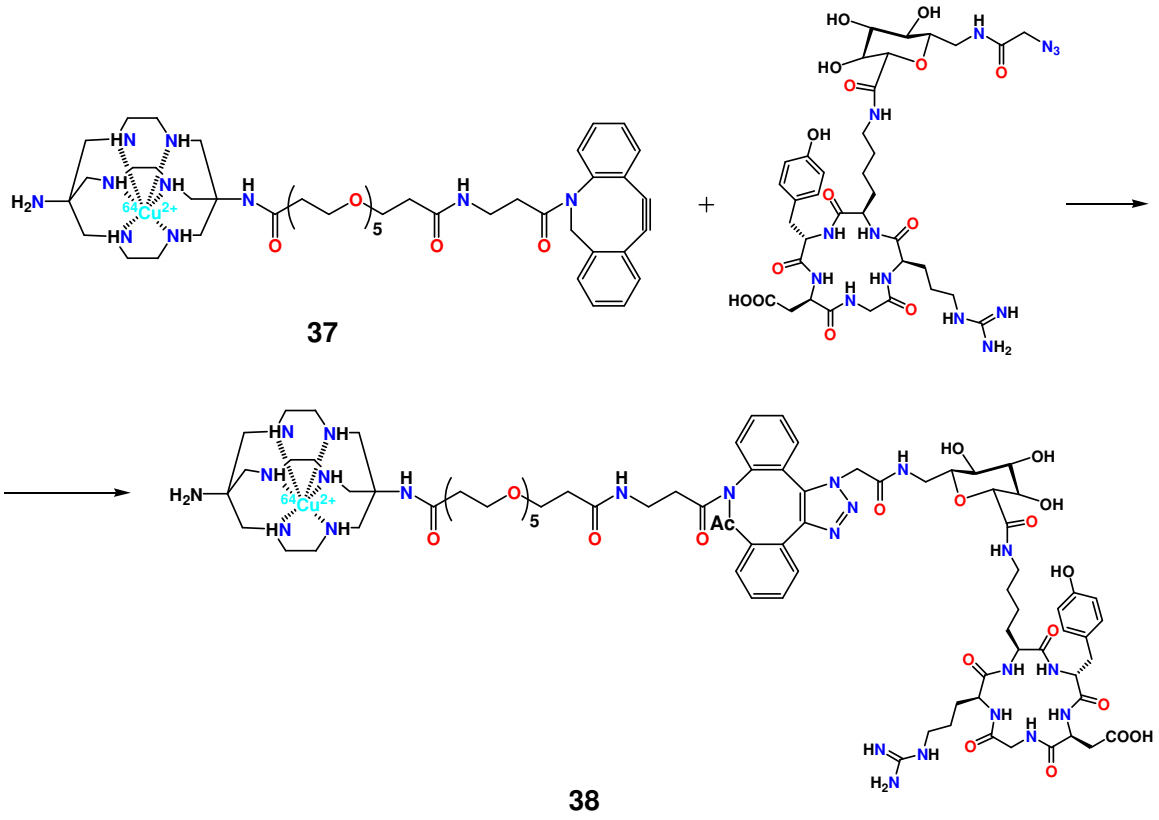

Scheme 11.Synthesis of sarcophaginate-based bioconjugate **38**.

Copper(II) sarcophaginates **41** and **42**, specifically designed for conjugation with antibodies [50], have been obtained from isothiocyanate-containing sarcophagines **39** and **40** (Scheme 12). According to *in vivo* biodistribution and PET imaging data, their ^{64}Cu-labelled radioimmunoconjugates with a HER2/neu-targeting antibody have shown high stability under physiological conditions with high and selective uptake in a HER2-positive cancer cell line. Cage complexes of homo- and heteromultifunctionalized sarcophagines **43** – **46** (Scheme 13) with the encapsulated $^{64}Cu^{2+}$ ion have also demonstrated good *in vitro* and *in vivo* stability [51], making these multifunctional chelators a versatile molecular platform for multivalent/multimodality probes for both imaging and therapy.

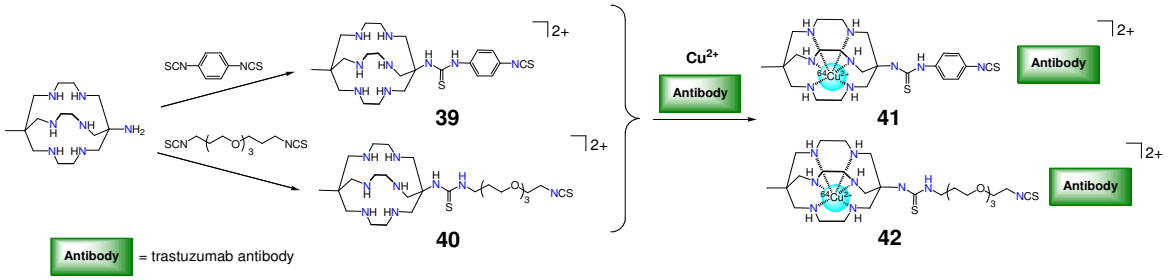

Scheme 12. Pathway to and functionalization of isothiocyanate-containing sarcophaginates **41** and **42**.

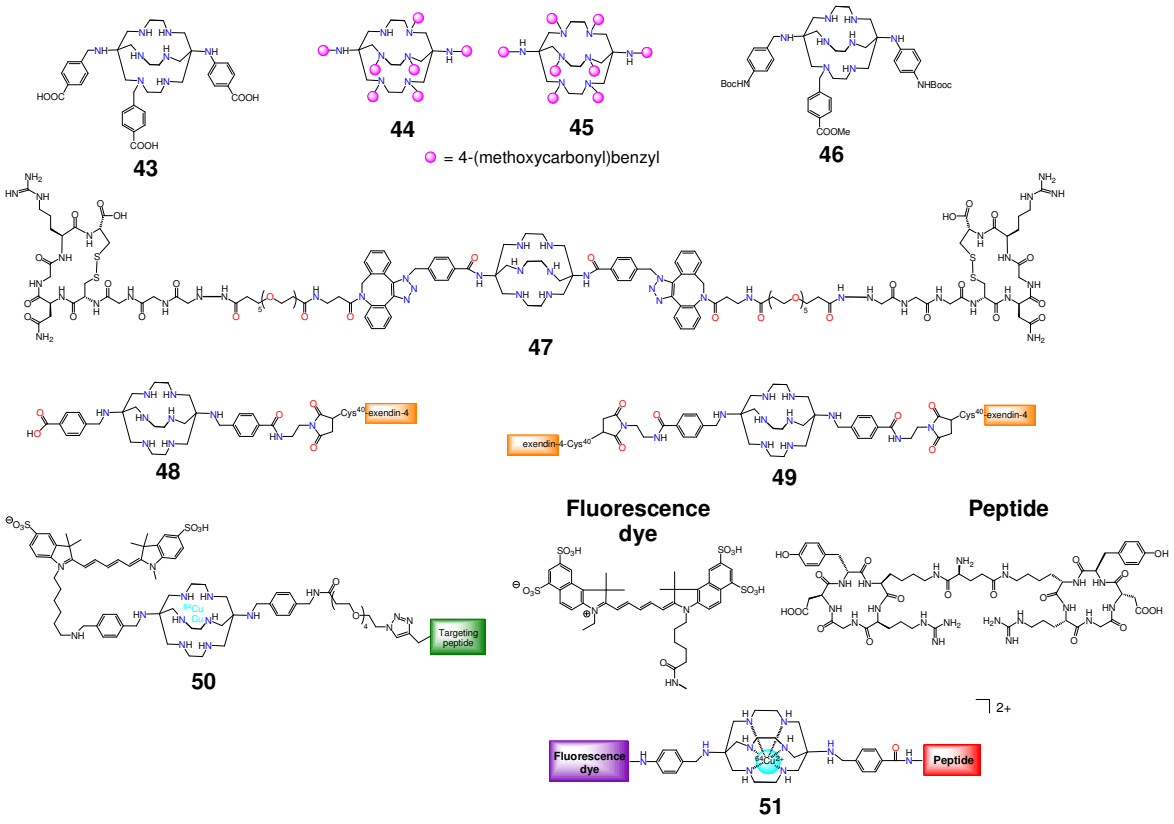

Scheme 13. Homo- and heterofunctionalized sarcophagine chelators for $^{64}Cu^{2+}$ cation.

A ^{64}Cu-labelled complex of a dipeptide sarcophagine **47** (Scheme 13), synthesized from a diazide-containing sarcophagine and a corresponding alkyne-containing peptide, has been used [52] for microPET imaging of the receptor CD13 (a tumor vasculature biomarker) expressed *in vitro* and *in vivo* in a living mice; it displayed a good binding affinity and CD13 specificity with given tumor cells and an excellent tumor uptake. Similarly, $^{64}Cu^{2+}$ cage complexes of exendin-4-functionalized sarcophagines **48** and **49**, having high kidney radioactivity levels [53], showed a persistent and specific uptake in a given insulinoma model; an increased tumor uptake *in vivo* has been also observed for **49**. These sarcophagines and their $^{64}Cu^{2+}$ complexes are, therefore, promising agents for 1-targeted PET imaging of the glucagon-like peptide. The receptor of this peptide with elevated expression profile in pancreatic islets, insulinoma and cardiovascular system [53] and its accurate visualization and quantification of β-cell mass are critical for improved understanding, diagnosis and treatment of type 1 diabetes and insulinoma.

A ^{64}Cu-labelled sarcophaginate **50** (Scheme 13), which contained a near-infrared fluorescent dye fragment and a peptide's exendin-4 moiety, has appeared to be suitable for bimodal PET–fluorescence imaging of the glucagon-like peptide 1 expression in pancreas and in pancreatic islet cell tumors [54]. It has demonstrated good performance *in vivo* and *ex vivo*, visualizing small xenografts with PET and pancreatic β-cell mass by phosphor autoradiography. Its

fluorescence has also allowed detecting individual pancreatic islets, thus confirming specific binding to a target peptide with the sensitivity surpassing that of a radioactive label. These dual imaging probes [54] can be used for the diagnosis of primary growths and metastases and for the detection of tumor margins, infiltrative growth and residual tumor cells. A heterofunctionalized sarcophaginate **51** [55] has also been proposed as a candidate for further design of various tumor-targeted dual-modality imaging probes.

Novel ^{64}Cu-labeled radiopharmaceuticals have been obtained from bifunctionalized sarcophagines **52** and **53** and their peptide-containing derivatives **54** and **55** (Scheme 14), which exhibited high tumor uptake and tumor-to-normal tissue ratios [56]. Triamidetriamine macrobicyclic and macrotricyclic ligands **56** and **57** for the delivery of the radioactive $^{64}Cu^{2+}$ ion (Scheme 15) have been synthesized [57] using a non-template synthetic strategy; the resulting $^{64}Cu^{2+}$ cage complex of **56** showed no signs of decomposition when incubated with L-cysteine and was rather stable in the presence of L-histidine as a concurrent *N*-donor ligand. The corresponding bifunctional sarcophagine has been conjugated with a tumor-targeting peptide Tyr3-octreotate to give a sarcophagine **58**. The corresponding $^{64}Cu^{2+}$ complex had high selectivity for tumor cells expressing somatostatin receptor 2 (sstr2) and an excellent uptake in sstr2-positive tumors, as shown both by *in vitro* and *in vivo* studies [58]. If labelled with $^{64}Cu^{2+}$ and $^{67}Cu^{2+}$ ions, the cage complex of **58** can be suitable for a combined imaging and therapeutic treatment of neuroendocrine tumors.

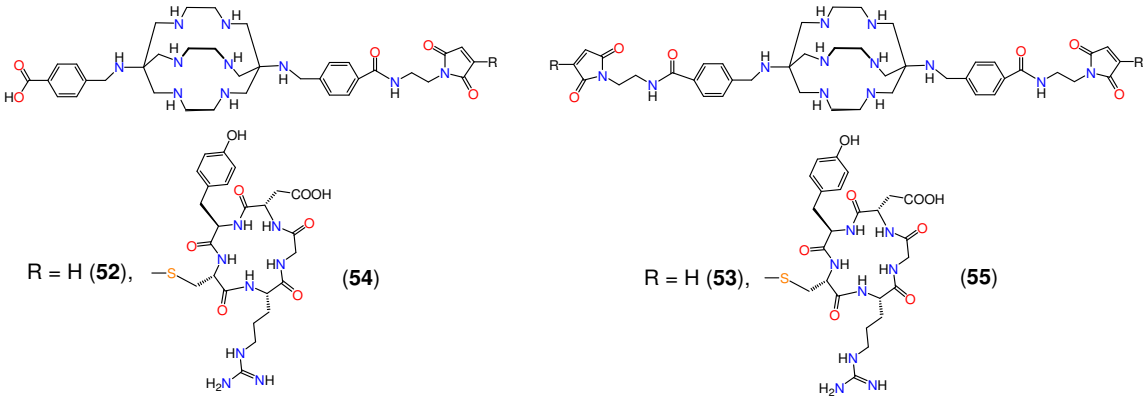

Scheme 14. Bifunctionalized sarcophagines **52** and **53** and their peptide-containing derivatives **54** and **55**.

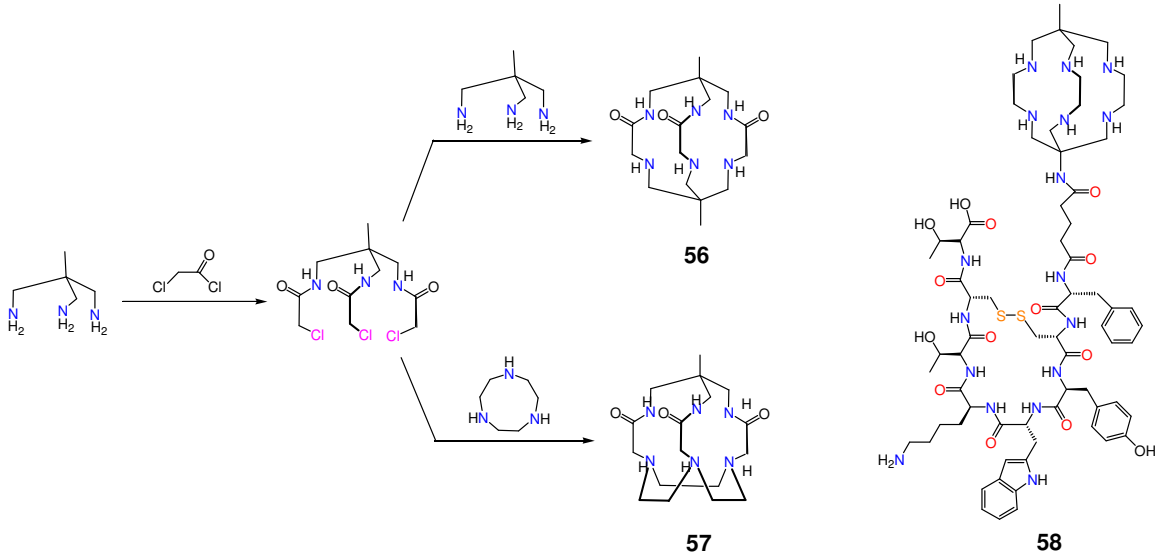

Scheme 15. Macrobi- and macrotricyclic ligands **56** and **57** and a peptide-functionalized sarcophagine **58**.

Conjugates of copper(II) sarcophaginates with antibodies, formed by suitable linkers (Scheme 16), have been proposed for target delivery of the $^{64}Cu^{2+}$ ions to a given biological system [59]. For example, the conjugate of a single-chain antibody with a monofunctionalized $^{64}Cu^{2+}$ sarcophaginate (Scheme 17) has been used for diagnostic PET imaging of activated platelets [60]. It accumulated in an injured vessel with high and specific uptake, thus paving the way towards highly sensitive *in vivo* detection of activated platelets and early diagnosis of acute thrombotic events [60].

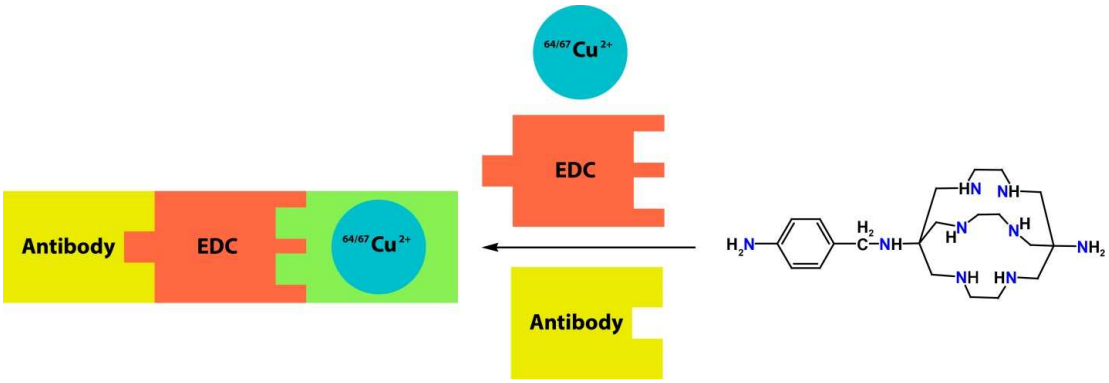

Scheme 16. Conjugation of $^{64}Cu^{2+}$ sarcophaginates with antibodies.

Similarly, a diagnostic potential for carotid artery thrombosis using PET has been demonstrated by a conjugate (Scheme 18) obtained *via* enzyme-mediated site-specific bioconjugation of a $^{64}Cu^{2+}$ sarcophaginate with a single-chain antibody [61]. A fragment of this antibody targeted the ligand-induced binding sites on a glycoprotein receptor GPIIb/IIIa found on

the activate platelets. The conjugate radiolabeled with the positron–emitting ^{64}Cu ions has been shown to selectively bind these platelets in an *in vivo* model.

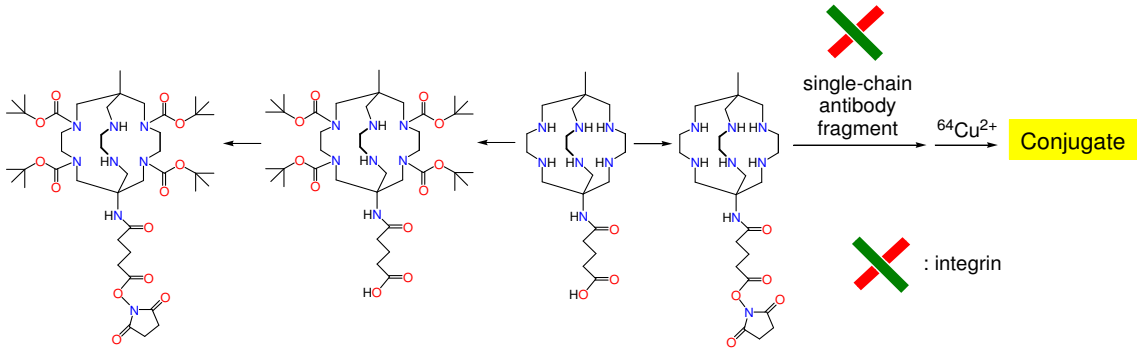

Scheme 17. Conjugate of a single-chain antibody with a monofunctionalized sarcophaginate.

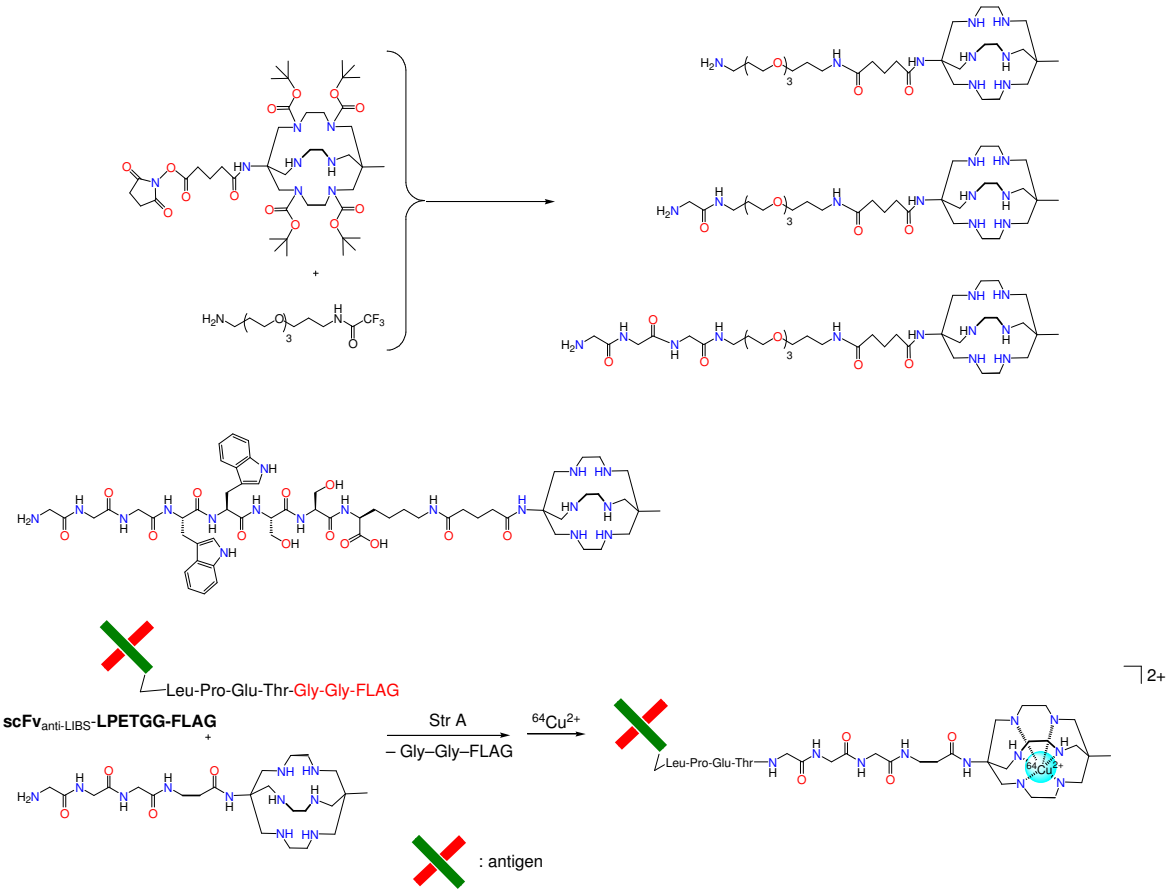

Scheme 18. Monofunctionalized sarcophagines and their conjugates with a single-chain antibody for $^{64}Cu^{2+}$ delivery.

A series of conjugates formed by eight different bifunctional sarcophagines (Scheme 19) has been probed for radiolabeling efficiency, *in vitro* stability and biodistribution [62]. Among those, a $^{64}Cu^{2+}$-label sarcophaginate **59** conjugated with an anti-CD20 antibody has appeared to be extremely stable *in vivo* and to achieve high specific activity under very dilute conditions. A

peptide-functionalized $^{64}Cu^{2+}$ sarcophaginate **60** [63] has also turned out to be an efficient probe for non-invasive PET imaging, in this case, of tumor-associated $\alpha_2\beta_1$ expression, thus being a useful tool for identifying prostate cancer.

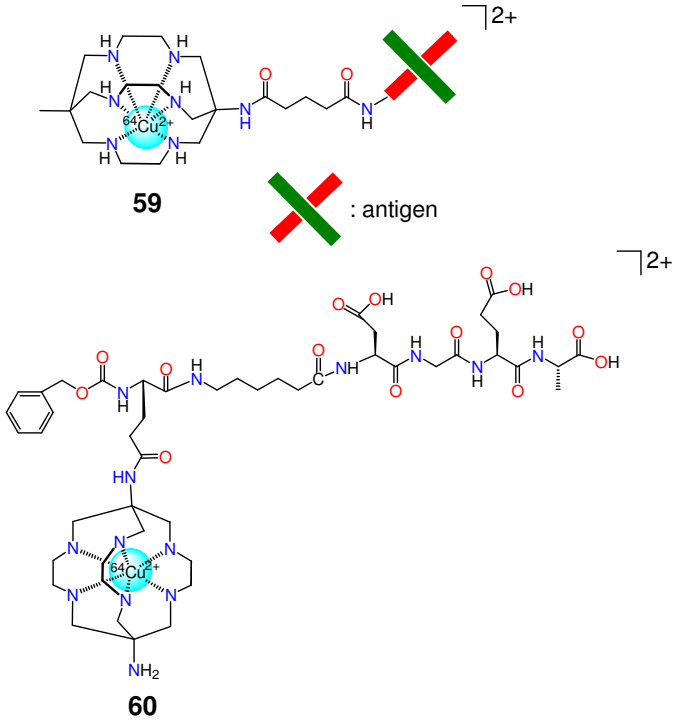

Scheme 19. $^{64}Cu^{2+}$-labelled conjugate **59** and a peptide-functionalized sarcophaginate **60**.

Heterobifunctionalized sarcophagines have also found use in design of long-circulating nanotherapeutics [64]. Nanoparticles formed by polypeptides modified by these $^{64}Cu^{2+}$ cage complexes *via* site-specific conjugation retained their activity *in vivo* over several days, and their kinetics can be followed by microPET imaging [64].

4. Cage complexes as paramagnetic probes for NMR and MRI applications

Nuclear magnetic resonance (NMR) and magnetic resonance imaging (MRI) have a well-deserved reputation as the most powerful techniques for studying biological systems. NMR spectroscopy is one of the main sources of information about their structural features; even being limited by the size of a biomacromolecule under study, it nevertheless allows determining its native conformation in a solution, thus ensuring continuing progress in this field.

One of possible approaches to increase the accuracy of structural information thus obtained is to use paramagnetic probes. Although most chemical applications of NMR spectroscopy consider the presence of paramagnetic species an unfortunate complication, both MRI and biological NMR often benefit from the effects they exert on magnetic properties of a system [65]. Paramagnetic labels, i.e. coordination compounds with paramagnetic transition metal or

lanthanide ions covalently attached to biological macromolecules, are gaining popularity as probes for NMR spectroscopy to help unraveling insightful details of structure and dynamics of proteins and their complexes. Some well-established applications of paramagnetic tags include NMR structure determination in solution [66], solid-state NMR crystallography [67] and characterization of otherwise inaccessible low-populated conformational states [68].

Paramagnetic probes make use of interactions of the spin of an unpaired electron with magnetic moments of the surrounding nuclei. An important feature of a paramagnetic ion is the electron relaxation time that is significantly shorter than the nuclear relaxation time. Slow electronic relaxation induces fast relaxation of nearby nuclei, thus resulting in a significant broadening of their NMR signals (so-called paramagnetic relaxation enhancement, PRE). Another feature is the magnetic anisotropy of a paramagnetic ion, which may result in very large paramagnetic shifts (so-called pseudocontact shifts, PCS) of NMR signals of the surrounding nuclei as well as in partial orientation of paramagnetic probes in the magnetic field giving rise to residual dipolar couplings (RDC). As all these effects depend on the coordinates of the corresponding nuclei in the molecular frame of a paramagnetic ion found in a relaxation or a shift agent, the data they provide contain detailed information about the structure and dynamics of a biomolecule.

MRI, which is unquestionably one of the most informative diagnostic techniques in modern medicine, also relies heavily on the paramagnetic probes. Differentiation of tissues from different organs is achieved by using inherent differences between relaxation times of water protons in different biological environments; this contrast may be enhanced even further by administering contrast (relaxation) agents, usually chelate complexes of gadolinium. A recently recognized adverse effect of gadolinium salts on certain groups of renally compromised patients, that is, causing nephrogenic systemic fibrosis [69], triggered an ongoing search for new contrast agents that were immune to transmetallation of the chelated gadolinium [70] or did not contain it at all.

Both paramagnetic shift and contrast agents require the highest possible stability of the paramagnetic species against loss of the metal ion, combined with their small overall size. Shift agents should also have large magnetic anisotropy to be effective, and contrast agents need to have an access of bulk water to the paramagnetic ion. All these seemingly conflicting conditions can be met if the metal ion is encapsulated in a three-dimensional cage; the most prominent example are gadofullerenes [71], in which the gadolinium cation or a charged metal-containing cluster is buried in a carbon cage [72]. In contrast to chelate-based contrast agents, it is almost impossible to lose the metal ion in this case, as it is trapped inside an impervious fullerene cage. Although usually such encapsulation would decrease relaxivity owing to the absence of direct

water-metal coordination that is necessary for inner-sphere relaxation, gadofullerenes have shown surprisingly high relaxivities [73] resulted from the formation of nanocluster aggregates [74] with large rotation correlation times. It makes the gadofullerenes more similar to nanoparticle-based contrast agents [75] rather than to molecular probes with all the associated limitations of the former, including limited ability to cross blood-brain barrier for brain tumor imaging. As the encapsulation in the gadofullerenes occurs not *via* chelation, they are beyond the scope of this short review; an interested reader is referred to excellent reviews on this topic [76].

Clathrochelates also have a fully encapsulated metal ion, thus ensuring their stability; however, the only report on their use as relaxation agents dates back to 1992 [77]. For manganese(II), copper(II) and chromium(III) sarcophaginates (**27**, **75** and **76** from Scheme 5), a modest relaxivity in simple aqueous solutions was found, which dramatically increased upon binding of the complex to a protein. This increase in relaxivity has been attributed to larger rotation correlation time of the protein, so it had the same nature as in the gadofullerenes. Also being redox-active and synthetically available, the transition metal clathrochelates can be therefore considered as worthy rivals to contrast agents based on the gadofullerenes, with which they share chemical stability and high relaxivity.

In the field of paramagnetic labels, lanthanide ion complexes also account for most of the labels available to date [78], as they have extremely large magnetic anisotropy, reasonably high chemical stability and tunable (by the choice of a specific lanthanide ion) paramagnetic behavior. Magnetic properties of the central ion govern the changes in chemical shifts, relaxation rates and weak alignment of a biomolecule in a magnetic field; all of those resulting in restrains useful for structure calculations [79]. Their further advancement is, however, hampered by high coordination number of lanthanide ions, large size of chelating probes, formation of several diastereomers [80] or conformational isomers [81] with different magnetic properties and by net positive charge of the probe [82].

Although 3d transition metal complexes have been the first to show have residual dipolar couplings [83], they are rarely considered as shift agents, as they usually have significantly lower magnetic anisotropy resulting in smaller paramagnetic pseudocontact shifts and lower alignment ability. Additionally, these complexes are often not stable enough owing to the oxidation of the central metal ion or its undesirable coordination, and the delocalization of unpaired electrons over the ligand leads to unwanted contact contribution to paramagnetic shifts that makes the interpretation of the experimental results even more difficult. As a result, the use of transition metal complexes is mostly limited to assessing natural metal-binding sites [84] or, in a chelated form, to their use as relaxation agents [85].

Clathrochelates eliminate most of the limitations caused by chemical stability or unwanted coordination; however, small (for low-spin cobalt(II) complexes [86]) or non-existent magnetic anisotropy precluded their use as shifting agents until recently. In 2010, it has been found that high-spin cobalt(II) tris-dioximate clathrochelates [87] with an unusual trigonal prismatic geometry had extremely large paramagnetic shifts in NMR spectra (Figure 2) and a very large anisotropy of the magnetic susceptibility, reaching as high as 12.6×10^{-32} m^3 at room temperature [12c]. Recently, the use of a tris-pyrazoloximate ligand allowed obtaining a cobalt(II) pseudo-clathrochelate [88] with the magnetic anisotropy that was even larger. The estimated value of 25×10^{-32} m^3 not only surpassed those for most of the lanthanide-based paramagnetic tags but also appeared to be enough to result in single-ion magnet behavior [89]. This shows a huge potential of the transition metal clathrochelates as new paramagnetic labels and contrast agents in biomolecular NMR and MRI, which, however, needs to be explored further for them to be placed into a toolkit of modern medicine.

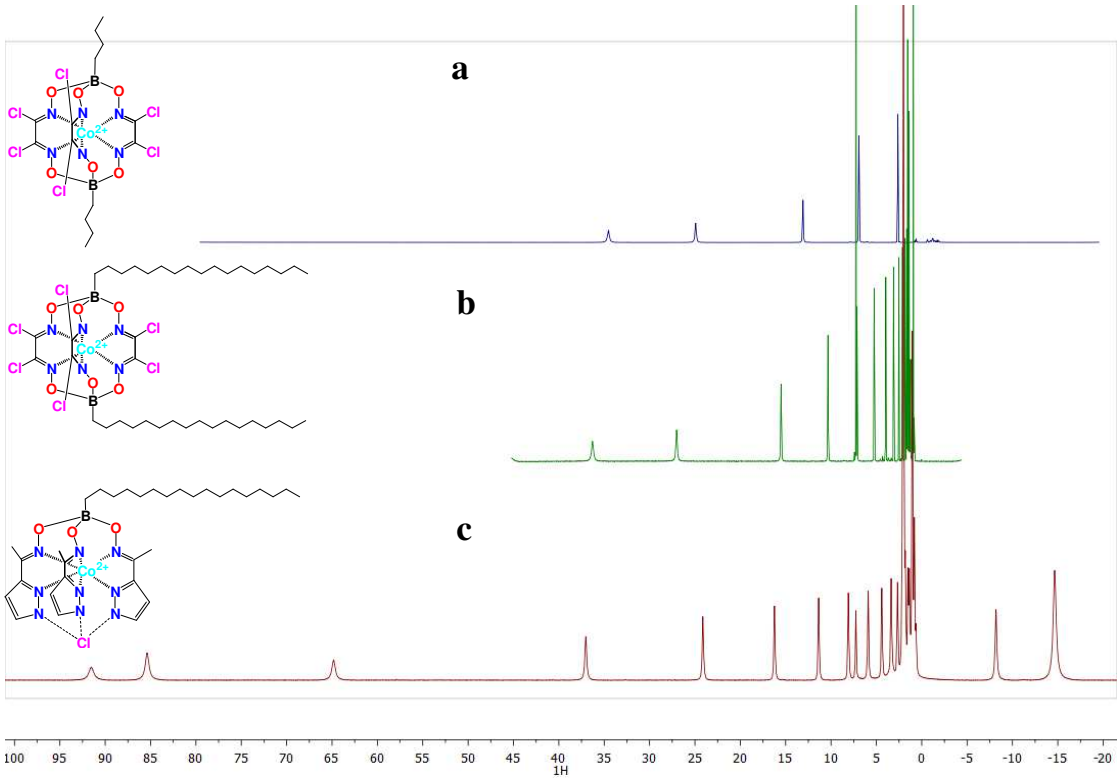

Figure 2. Paramagnetically-shifted ^{1}H NMR spectra of high-spin cobalt(II) clathrochelates (**a** and **b**) and a hexadecylboron-capped pseudoclathrochelate (**c**).

5. Conclusion

Metal complexes have long found use in many areas of material and medicinal sciences, yet new ones are still emerging every day. In this short review, we have briefly covered the recent

progress in a fast developing area of biological applications of a unique type of the complexes with an encapsulated metal ion, the clathrochelates. In contrast to many reported metal-containing therapeutic and diagnostic agents, for these cage compounds it is possible to clearly demarcate biologically relevant properties evoked by the encapsulated metal ion (such as radioactive and magnetic properties) and those governed by ligand-related size-and-shape features. While some of the reviewed complexes (e.g. radiotherapeutic agents) are on the verge to enter clinical trials, medicinal applications of others are still to emerge.

Acknowledgements

The authors acknowledge the Russian Science Foundation (project 14-13-00724) for financial support.

References

1. (a) Z.J. Lesnikowski, *Curr. Org. Chem.* 2007, **11**, 355–381; (c) A.M. Chad, T.A. Taton, *Nature,* 2000, **405**, 626–627; (b) A.S. Abd-El-Aziz, C.E Carraher, C.U. Pittman, J.E. Sheats, M. Zeldin, *Macromolecules Containing Metal and Metal-Like Elements. Biomedical Applications.,* Vol. 3, Wiley-Interscience, 2004.

2. (a) S.P. Fricker, *Dalton.Trans.*, 2007, 4903–4917; (b) K.J. Kilpin, P.J. Dyson, *Chem.Sci.*, 2013, **4**, 1410–1419; (c) N.P.E. Barry, P.J. Sadler, *Chem. Commun*., 2013, **49**, 5106–5131; (d) M. Dörr, E. Meggers, *Curr. Opin. Chem. Biol*. 2014, **19**, 76–81.

3. (a) E. Meggers, *Chem. Commun*., 2009, 1001–1010; (b) E.Meggers, *Angew. Chem. Int. Ed.*, 2012, **51**, 1–4.

4. M. Corsini, F. Fabrizi de Biani, P. Zanello, *Coord. Chem. Rev*., 2006, **250**, 1351–1372.

5. D.-L.Ma, H.-Z.He, K.-H.Leung, D.S.-H.Chan, C.-H.Leung, *Angew. Chem. Int. Ed*., 2013, **52**, 7666–7682.

6. A.L. Noffke, A. Habtemariam, A.M. Pizarro, P.J.Sadler, *Chem.Comm*, 2012, **48**, 5219–5246.

7. (a) V. Amendola, *Coord. Chem. Rev*., 2006, **250**, 1451–1470; (b) P.S. Donnelly, *Dalton Trans*., 2011, **40**, 999–1010.

8. R. B. Lauffer, *Chem. Rev*., 1987, **87**, 901–927.

9. P.K. Sasmal, C.N. Streu, E.Meggers, *Chem.Comm*, 2013, **49**, 1581–1587.

10. Y.Z. Voloshin, N.A. Kostromina, R. Krämer, *Clathrochelates: synthesis, structure and properties*, Elsevier, Amsterdam, 2002.

11. S. Viswanathan, Y.Z. Voloshin, H. Radecka, J. Radecki, *Electrochim. Acta*, 2009, **54**, 5431–5438.

12. (a) V.V. Novikov, I.V. Ananyev, A.A. Pavlov, M.V. Fedin, K.A. Lyssenko, Y.Z. Voloshin, *J. Phys. Chem. Lett*., 2014, **5**, 496–500; (b) M. Azarkh, L. Penkova, S. Kats, O. Varzatskii, Y. Voloshin, E. Groenen, *J. Phys. Chem. Lett.*, 2014, **5**, 886−889; (c) V.V. Novikov, A.A. Pavlov, A.S. Belov, A.V. Vologzhanina, A. Savitsky, Y.Z. Voloshin, *J. Phys. Chem. Lett*., 2014, **5**, 3799–3803.

13. A.B. Burdukov, M.A. Vershinin, N.V. Pervukhina, E.G. Boguslvaskii, I.V. Eltsov, L.A. Shundrin, S.L. Selector, A.V. Shokurov, Y.Z. Voloshin, *Inorg. Chem. Com.*, 2014, **44**, 183–187.

14. (a) Y.Z. Voloshin, O.A. Varzatskii, M.Y. Antipin, S.V. Korobko, V.Y. Chernii, S.V. Volkov, V.I. Pehn'o, Z.A. Starikova, *Inorg. Chem*., 2005, **44**, 822–824; (b) J.R. Sabin, O.A. Varzatskii, Y.Z. Voloshin, Z.A. Starikova, V.V. Novikov, V.N. Nemykin, *Inorg. Chem.,* 2012, **51**, 8362−8372.

15. (a) O. Pantani, S. Naskar, R. Guillot, M. Millet, E. Anxolabéhère-Mallart, A. Aukauloo, *Angew. Chem., Int. Ed*., 2008, **47**, 9948–9950; (b) Y.Z. Voloshin, A.V. Dolganov, O.A. Varzatskii, Y.N. Bubnov, *Chem. Commun*., 2011, **47**, 7737–7739; (c) M.T.D. Nguyen, M.-F. Charlot, A. Aukauloo, *J. Phys. Chem. A*, 2011, **115**, 911–922; (d) P. Millet, N. Mbemba, S.A. Grigoriev, V.N. Fateev, A. Aukauloo, C. Etiévant, *Int. J. Hydr. Energy*., 2011, **36**, 4134–4142; (e) Y.Z. Voloshin, A.S. Belov, A.V. Vologzhanina, G.G. Aleksandrov, A.V. Dolganov, V.V. Novikov, O.A. Varzatskii, Y.N. Bubnov, *Dalton Trans*., 2012, **41**, 6078–6093; (f) E. Anxolabéhère-Mallart, C. Costentin, M. Fournier, S. Nowak, M. Robert and J.-M.Savéant, *J. Am. Chem. Soc.*, 2012, **134**, 6104–6107; (g) A.V. Dolganov, A.S. Belov, V.V. Novikov, A.V. Vologzhanina, A. Mokhir, Y.N. Bubnov and Y.Z. Voloshin, *Dalton Trans*., 2013, **42**, 4373–4376; (h) I.G. Belaya, S.V. Svidlov, A.V. Dolganov, G.E. Zelinskii, T.V. Potapova, A.V. Vologzhanina, O.A. Varzatskii, Y.N. Bubnov, Y.Z. Voloshin, *Dalton Trans*., 2013, **42**, 13667–16678; (i) A.V. Dolganov, I.G. Belaya, Y.Z. Voloshin, *Electrochim. Acta*, 2014, **125**, 302–306.

16. (a) Y.-Y. Zhang, Y.-J. Lin, G.-X. *Chem. Commun*., 2014, **50**, 2327–2329; (b) M.D. Wise, A. Ruggi, M. Pascu, R. Scopelliti, K. Severin, *Chem. Sci*., 2013, **4**, 1658–1662.

17. M.D. Wise, J.J. Holstein, P. Pattison, C. Besnard, E. Solari, R. Scopelliti, G. Bricogne, K. Severin, *Chem. Sci*., 2015, **6**, 1004–1010.

18. A.M. Sargeson, *Coord. Chem .Rev*., 1996, **151**, 89–114.

19. Y.Z. Voloshin, O.A. Varzatskii, Yu.N. Bubnov, *Rus. Chem. Bul. Int. Ed*., 2007, **56**, 577–605.

20. K. Gunasekaran, B. Ma, R. Nussinov, *Proteins*, 2004, **57**, 433–443.

21. Y. Voloshin, O. Varzatskii, S. Shul'ga, V. Novikov, A. Belov, I. Makarenko, I. Dubey, D. Krivorotenko, V. Negrutska, K. Zhizhin, N. Kuznetsov, Y. Bubnov, *Proc. 10th EUROBIC*, 2010, 29–38.

22. E. Meggers, *Angew. Chem. Int. Ed.*, 2011, **50**, 2442–2448.

23. R. Bakry, R.M. Vallant, M. Najam-ul-Haq, M. Rainer, Z. Szabo, C.W. Huck, G.K. Bonn, *Int. J. Nanomedicine*, 2007, **24**, 639–649.

24. (a) R.N. Grimes, *Carboranes,* 2nd ed., Academic Press, 2011; (b) N.S. Hosmane ed., *Boron Sciences. New technologies and Applications*, CRC Press, 2011; (c) N.S. Hosmane, J.A. Maguire, Z. Yinghuai, M. Takagaki, *Boron and Gadolinium Neutron Capture Therapy for Cancer Treatment*, World Scientific Publishers, 2012; (d) J. Poater, M. Sola, C. Vinas, F. Teixidor, *Angew. Chem. Int. Ed*., 2014, **53,** 12191–12195; (e) Z.J. Leśnikowski*, Coll. Czech. Chem. Commun.,* 2007, **72**, 1646–1658; (f) F. Issa, M. Kassiou, L.M. Rendina, *Chem. Rev*., 2011, **111,** 5701; (g) M. Scholz, E. Hey-Hawkins, *Chem. Rev*., **111**,7035-62.

25. (a) C.E. Wagner, M.L. Mohler, G.S. Kang, D.D. Miller, E.E. Geisert, Y.-A. Chang, E.B. Fleischer, K.J. Shea, *J. Med. Chem*., 2003, **46**, 2823–2833 and references therein; (b) I. Papanastasiou, A. Tsotinis, N. Kolocouris, S. R. Prathalingam, J.M. Kelly, *J. Med. Chem*., 2008, **51**, 1496–1500 and references therein.

26. (a) Y.Z. Voloshin, O.A. Varzatskii, A.V. Palchik, I.I. Vorontsov, M.Yu. Antipin, E.G. Lebed, *Inorg. Chim. Acta*, 2005, **358**, 131–146; (b) Y.Z. Voloshin, O.A. Varzatskii, A.V. Palchik, Z.A. Starikova, M.Yu. Antipin, E.G. Lebed, Y.N. Bubnov, *Inorg. Chim. Acta,* 2006, **359**, 553–569; (c) A.S. Belov, A.V. Vologzhanina, V.V. Novikov, V.V. Negrutska,

I.Y. Dubey, Z.A. Mikhailova, E.G. Lebed, Y.Z. Voloshin, *Inorg. Chim. Acta*, 2014, **421**, 300–306.

27. (a) Y.Z. Voloshin, V.E. Zavodnik, O.A. Varzatskii, V.K. Belsky, A.V. Palchik, N.G. Strizhakova, I.I. Vorontsov, M.Yu. Antipin, *J. Chem. Soc., Dalton Trans*., 2002, 1193–1202; (b) Y.Z. Voloshin, O.A. Varzatskii, P.A. Stuzhin, S.V. Shul'ga, S.V. Volkov, A.V. Vologzhanina, E.G. Lebed, Y.N. Bubnov, *Inorg. Chem. Comm*., 2011, **14**, 1504–1507; (c) Y.Z. Voloshin, O.A. Varzatskii, S.V. Shul'ga, I.N. Denisenko, A.V. Vologzhanina, Y.N. Bubnov, *Inorg. Chem. Com*., 2012, **17**, 128–131; (d) O.A. Varzatskii, I.N. Denisenko, S.V. Volkov, A.V. Dolganov, A.V. Vologzhanina, Y.N. Bubnov, Y.Z. Voloshin, *Inorg. Chem. Commun*., 2013, **33**, 147–150; (e) O.I. Artyushin, I.L. Odinets, E.V. Matveeva, A.V. Vologzhanina, O.A. Varzatskii, S.E.Lubimov, Y.Z. Voloshin, *Dalton Trans.*, 2014, **43**, 9677–9689; (f) O.A. Varzatskii, I.N. Denisenko, A.S. Belov, A.V. Vologzhanina, Y.N. Bubnov, S.V. Volkov, Y.Z. Voloshin, *Inorg. Chem. Commun*., 2014, **44**, 134–138.

28. (a) Y.Z. Voloshin, O.A. Varzatskii, T.E. Kron, V.K. Belsky, V.E. Zavodnik, N.G. Strizhakova, A.V. Palchik, *Inorg. Chem*. 2000, **39**, 1907–1918; (b) Y.Z. Voloshin, O.A. Varzatskii, T.E. Kron, V.K. Belsky, V.E. Zavodnik, N.G. Strizhakova, V.A. Nadtochenko, V.A. Smirnov, *J. Chem. Soc., Dalton Trans*., 2002, 1203–1211; (c) Y.Z. Voloshin, O.A. Varzatskii, I.N. Denisenko, S.V. Volkov, A.S. Belov, A.V. Dolganov, A.V. Vologzhanina, V.V. Novikov, Y.N. Bubnov, *Eur. J. Inorg. Chem.*, 2013, 3178–3184; (d) A.V. Dolganov, A.S. Belov, V.V.Novikov, A.V. Vologzhanina, G.V. Romanenko, Y.G. Budnikova, G.E. Zelinskii, M.I. Buzin, Y.Z. Voloshin, *Dalton Trans*., 2014, **44**, 2476–2487.

29. M.Y. Losytskyy, V.B. Kovalska, O.A. Varzatskii, A.M. Sergeev, S.M. Yarmoluk, Y.Z. Voloshin, *J. Fluoresc.*, 2013, **23**, 889–895.

30. G.R. Bardajee, Z. Hooshyar, P. Shafagh, S. Ghiasvand, N. Kakavand, *J. Luminesc*., 2014, **156**, 55–62.

31. Z. Hooshyar, G.R. Bardajee, P. Shafagh, S. Ghiasvand, M. Khanjari, N. Dianatnejad, *J. Iran. Chem. Soc*., 2015, **12**, 715–725.

32. Z. Hooshyar, G.R. Bardajee; N. Kakavand, M. Khanjari, N. Dianatnejad, *Luminesc.*, 2014, DOI: 10.1002/bio.2773.

33. Y.Z. Voloshin, O.A. Varzatskii, V.V. Novikov, Y.N. Bubnov, *Proc. 9th EUROBIC*, 2008, 71–76.

34. (a) V.V. Novikov, O.A. Varzatskii, V.V. Negrutska, Y.N. Bubnov, L.G. Palchykovska, I.Y. Dubey, Y.Z. Voloshin, *J. Inorg. Biochem.,* 2013, **124**, 42–45; (b) Y.Z. Voloshin, V.V. Novikov, O.A. Varzatskii, V.V. Negrutska, L.G. Palchykovska, I.Y. Dubey, Y.N. Bubnov, Patent RU 2012/106191.

35. P. Cigler, M. Kozisek, P. Rezacova, J. Brynda, Z. Otwinowski, J. Pokorna, J. Plesek, B. Gruner, L. Doleckova-Maresova, M. Masa, J. Sedlacek, J. Bodem, H. G. Krausslich, V. Kral, J. Konvalinka, *Proc. Natl. Acad. Sci. USA*, 2005, **102**, 15394–15399.

36. M. Kozisek, P. Cigler, M. Lepsik, J. Fanfrlik, P. Rezacova, J. Brynda, J. Pokorna, J. Plesek, B. Gruner, K. Grantz Saskova, J. Vaclavikova, V. Kral, J. Konvalinka, *J. Med. Chem*., 2008, **51**, 4839–4843.

37. (a) O.A. Varzatskii, V.V. Novikov, S.V. Shulga, A.S. Belov, A.V. Vologzhanina, V.V. Negrutska, I.Y. Dubey, Y.N. Bubnov, Y.Z. Voloshin, *Chem. Commun*., 2014, **50**, 3166–3168; (b) O.A. Varzatskii, S.V. Shul'ga, A.S. Belov, V.V. Novikov, A.V. Dolganov, A.V. Vologzhanina, Y.Z. Voloshin, *Dalton Trans*., 2014, **43**, 17934–17948.

38. V.B. Kovalska, M.Yu. Losytskyy, O.A. Varzatskii, V.V. Cherepanov, Y.Z. Voloshin, A.A. Mokhir, S.M. Yarmoluk, S.V. Volkov, *Bioorgan. Med. Chem*., 2014, **22**, 1883–1888.

39. H. Deng, V.A. Bloomfield, *Biophysic. J.*, 1999, **77**, 1556–1561.

40. (a) D.L. Bailey, D.W. Townsend; P.E. Valk; M.N. Maisey. *Positron Emission Tomography: Basic Sciences*. Secaucus, NJ: Springer, 2005; (b) P.S. Donnelly, *Dalton Trans*., 2011, **40**, 999–1010; (c) V. Amendola, *Coord. Chem. Rev*., 2006, **250**, 1451–1470.

41. P.J. Blower, J.S. Lewis, J. Zweit, *Nucl. Med. Biol*., 1996, **23**, 957–980.

42. (a) S.V. Smith, *J. Inorg. Biochem*., 2004, **98**, 1874–1901; (b) N.Di Bartolo, A.M. Sargeson, S.V. Smith, *Org. Biomol. Chem*., 2006, **4**, 3350–3357; (c) S.D. Voss, S.V. Smith, N.Di Bartolo, L.J. McIntosh, E.M. Cyr, A.A. Bonab, E.A. Carter, A.J. Fischman, S.T. Treves, S.D. Gillies, A.M. Sargeson, J.S. Huston, A.B. Packard, *Proc. Natl. Acad. Sci. USA,* 2007, **104**, 17489–17493.

43. H. Cai, J. Fissekis, P.S. Conti, *Dalton Trans*., 2009, 5395–5400.

44. H. Cai, Z. Li, C.-W. Huang, R. Park, A.H. Shahinian, P.S. Conti, *Nucl. Med. Biol*., 2010, **37**, 57–65.

45. S. Liu, Z. Li, L.-P. Yap, C.-W. Huang, R. Park, P.S. Conti, *Chem. Eur. J*., 2011, **17**, 10222–10225.

46. M.T. Ma, O.C. Neels, D. Denoyer, P. Roselt, J.A. Karas, D.B. Scanlon, J.M. White, R.J. Hicks, P.S. Donnelly, *Bioconjugate Chem*., 2011, **22**, 2093–2103.

47. M.T. Ma, J.A. Karas, J.M. White, D. Scanlon, P.S. Donnelly, *Chem. Commun*., 2009, 3237–3239.

48. M.T. Ma, M.S. Cooper, R.L. Paul, K.P. Shaw, J.A. Karas, D. Scanlon, J.M. White, P.J. Blower, P.S. Donnelly, *Inorg. Chem*., 2011, **50**, 6701–6710.

49. K. Chen, X. Wang, W.-Y. Lin, C. K.-F. Shen, L.-P. Yap, L.D. Hughes, P.S. Conti, *ACS Med. Chem. Lett.*, 2012, **3**, 1019–1023.

50. B.M. Paterson, G. Buncic, L.E. McInnes, P. Roselt, C. Cullinane, D.S. Binns, C.M. Jeffery, R.I. Price, R.J. Hicks, P.S. Donnelly, *Dalton Trans*., 2015, **44**, 4901–4909.

51. S. Liu, Z. Li, P.S. Conti, *Molecules*, 2014, **19**, 4246–4255.

52. G. Li, X. Wang, S. Zong, J. Wang, P.S. Conti, K. Chen, *Molecular Pharmaceutics*, 2014, **11**, 3938–3946.

53. Z. Wu, S. Liu, I. Nair, K. Omori, S. Scott, I. Todorov, J.E. Shively, P.S. Conti, Z. Li, F. Kandeel, *Theranostics,* 2014, **4**, 770–777.

54. C. Brand, D. Abdel-Atti, Y. Zhang, S. Carlin, S.M. Clardy, E.J. Keliher, W.A. Weber, J.S. Lewis, T. Reiner, *Bioconjugate Chemistry*, 2014, **25**, 1323–1330.

55. S. Liu, D. Li, C.-W. Huang, L.-P. Yap, R. Park, H. Shan, Z. Li, P.S. Conti, *Mol. Imag. Biol.*, 2012, **14**, 718–724.

56. S. Liu, D. Li, C.-W. Huang, L.-P. Yap, R. Park, H. Shan, Z. Li, P.S. Conti, *Theranostics*, 2012, **2**, 589–596.

57. K.V. Tan, P.A. Pellegrini, B.W. Skelton, C.F. Hogan, I. Greguric, P.J. Barnard, *Inorg. Chem*., 2014, **53**, 468–477.

58. B.M. Paterson, P. Roselt, D. Denoyer, C. Cullinane, D. Binns, W. Noonan, C.M. Jeffery, R.I. Price, J.M. White, R.J. Hicks, P.S. Donnelly, *Dalton Trans.*, 2014, **43**, 1386–1396.

59. S.V. Smith, J.M. Harrowfield, N.M. Di Bartolo, A.M. Sargeson, *PCT Int. Appl. WO 00 40*, 585 (Cl. C07D487/08) Publ. 13.07.2000.

60. K. Alt, B.M. Paterson, K. Ardipradja, C. Schieber, G. Buncic, B. Lim, S.S. Poniger, B. Jakoby, X. Wang, G. J. O'Keefe, H.J. Tochon-Danguy, A.M. Scott, U. Ackermann, K. Peter, P.S. Donnelly, C.E. Hagemeyer, *Molecular Pharmaceutics*, 2014, **11**, 2855–2863.

61. B.M. Paterson, K. Alt, C.M. Jeffery, R.I. Price, S. Jagdale, S. Rigby, C.C. Williams, K. Peter, C.E. Hagemeyer, P.S. Donnelly, *Angew. Chem. Int. Ed*., 2014, **53**, 6115–6119.

62. M.S. Cooper, M.T. Ma, K. Sunassee, K.P. Shaw, J.D. Williams, R.L. Paul, P. S. Donnelly, P.J. Blower, *Bioconjugate Chem.*, 2012, **23**, 1029–1039.

63. C.-W. Huang, Z. Li, H. Cai, K. Chen, T. Shahinian, P.S. Conti, *Eur.J. Nucl. Med. Mol. Imag.*, 2011, **38**, 1313–1322.

64. S.M. Janib, S. Liu, R. Park, M.K. Pastuszka, P. Shi, A.S. Moses, M.M. Orosco, Y.-A. Lin, H. Cui, P.S. Conti, *Integrative Biology,* 2013, **5**, 183–194.

65. I. Bertini, C. Luchinat, G. Parigi, *Solution NMR of paramagnetic molecules: applications to metallobiomolecules and models*. Elsevier: 2001, Vol. 2.

66. M.A. Hass, M. Ubbink, *Curr. Opin. Struct. Biol*., 2014, **24**, 45–53.

67. C. Luchinat, G. Parigi, E. Ravera, M. Rinaldelli, *J. Am. Chem. Soc*., 2012, **134**, 5006–5009.

68. J. Iwahara, G.M. Clore, *Nature*, 2006, **440**, 1227–1230.

69. T. Grobner, F.C. Prischl, *Kidney Int*., 2007, **72**, 260–264.

70. D.E. Sosnovik, P.Caravan, *Curr. Cardiovasc. Imaging. Rep*., 2013, **6**, 61–68.

71. R.D. Bolskar, *Nanomedicine (Lond),* 2008, **3**, 201–213.

72. X. Lu, L. Feng, T. Akasaka, S. Nagase, *Chem. Soc. Rev*., 2012, **41**, 7723–7760.

73. É. Tóth, R.D. Bolskar, A. Borel, G. González, L. Helm, A.E. Merbach, B. Sitharaman, L.J. Wilson, *J. Am. Chem. Soc*., 2005, **127**, 799–805.

74. (a) S. Laus, B. Sitharaman, É. Tóth, R.D. Bolskar, L. Helm, L.J. Wilson, A.E. Merbach, *J. Phys. Chem*. C, 2007, **111**, 5633–5639; (b) S. Laus, B. Sitharaman, É. Tóth, R.D. Bolskar, L. Helm, S. Asokan, M.S. Wong, L.J. Wilson, A.E. Merbach, *J. Am. Chem. Soc*., 2005, **127**, 9368–9369.

75. C. Felton, A. Karmakar, Y. Gartia, P. Ramidi, A.S. Biris, A. Ghosh, *Drug Metab. Rev*., 2014, **46**, 142–154.

76. (a) R.D Bolskar, *Nanomedicine*, 2008, **3**, 201–221; (b) P.P. Fatouros, M.D. Shultz, *Nanomedicine (Lond)*, 2013, **8**,1853–1864.

77. L.S. Szczepaniak, A. Sargeson, I.I. Creasei, R.J. Geue, M. Tweedle, R.G. Bryant, *Bioconjugate Chem*., 1992, **3**, 27–31.

78. W.-M. Liu, M. Overhand, M. Ubbink, *Coord. Chem. Rev*., 2014, **273**–**274**, 2–12.

79. G. Otting, *Annu. Rev. Biophys*. 2010, **39**, 387–405.

80. G. Pintacuda, A. Moshref, A. Leonchiks, A. Sharipo, G. Otting, *J. Biomol. NMR,* 2004, **29**, 351–361.

81. M. Prudencio, J. Rohovec, J.A. Peters, E. Tocheva, M.J. Boulanger, M.E.P. Murphy, H.J. Hupkes, W. Kosters, A. Impagliazzo, M. Ubbink, *Chem. Eur. J*., 2004, **10**, 3252–3260.

82. P.H.J. Keizers, J.F. Desreux, M. Overhand, M. Ubbink, *J. Am. Chem. Soc.,* 2007, **129**, 9292–9293.

83. A.A. Bothner-By, P.J. Domaille, C. Gayathri, *J. Am. Chem. Soc*., 1981, **103**, 5602–5603.

84. M. Piccioli, P. Turano, *Coord. Chem. Rev*., 2015, **284**, 313–328.

85. R.B. Lauffer, *Chem. Rev*., 1987, **87**, 901–927.

86. Y.Z. Voloshin, A.Y. Lebedev, V.V. Novikov, A.V. Dolganov, A.V. Vologzhanina, E.G. Lebed, A.A. Pavlov, Z.A. Starikova, M.I. Buzin, Y.N. Bubnov, *Inorg. Chim. Acta*, 2013, **399**, 67 – 78.

87. Y.Z. Voloshin, O.A. Varzatskii, V.V. Novikov, N.G. Strizhakova, I.I. Vorontsov, A.V. Vologzhanina, K.A. Lyssenko, G.V. Romanenko, M.V. Fedin, V.I. Ovcharenko, Y.N. Bubnov, *Eur. J. Inorg. Chem.*, 2010, 5401–5415.

88. O.A. Varzatskii, L.V. Penkova, S.V. Kats, A.V. Dolganov, A.V. Vologzhanina, A.A.Pavlov, V.V. Novikov, A.S. Bogomyakov, V.N. Nemykin, Y.Z. Voloshin, *Inorg. Chem.*, 2014, **53**, 3062–3071.

89. V.V. Novikov, A.A. Pavlov, Yu.V. Nelyubina, M.-E. Boulon, O.A. Varzatskii, Ya.Z. Voloshin, R.E.P. Winpenny, *J. Am. Chem. Soc.*, 2015, 10.1021/jacs.5b05739.